

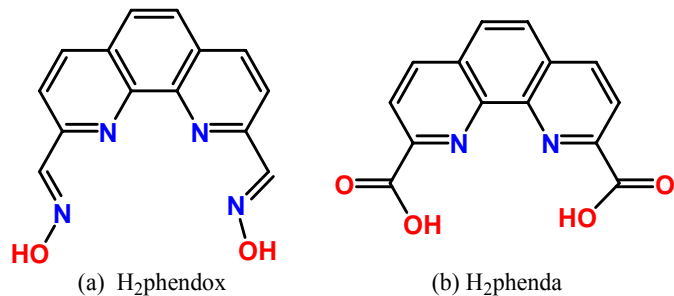
Supporting Information for

Chloride Tempered Formation of $\{\text{Dy}_{12}(\text{OH})_{16}\}^{20+}$ Cluster Core Incorporating 1,10-phenanthroline-2,9-dicarboxylate

Yan-Li Miao,^{a,b} Jun-Liang Liu,^a Ji-Dong Leng^a, Zhuo-Jia Lin,^a and Ming-Liang Tong^{*a}

^a Key Laboratory of Bioinorganic and Synthetic Chemistry of Ministry of Education / State Key Laboratory of Optoelectronic Materials and Technologies, School of Chemistry and Chemical Engineering, Sun Yat-Sen University, Guangzhou 510275, China. E-mail: tongml@mail.sysu.edu.cn

^b College of Science, Guangdong Ocean University, Zhanjiang 524088, P. R. China



Scheme S1 1,10-phenanthroline-2,9-dicarbaldehyde dioxime (H₂phendox) and 1,10-phenanthroline-2,9-dicarboxylic acid (H₂phenda).

Experimental Section

Materials and Physical Measurements. The reagents and solvents employed were commercially available and used as received without further purification. The ligands 1,10-Phenanthroline-2,9-dicarbaldehyde dioxime (H₂phendox) and 1,10-phenanthroline-2,9-dicarboxylic acid (H₂phenda)

were synthesized according to a literature method.¹ The C, H, and N microanalyses were carried out with an Elementar Vario-EL CHNS elemental analyzer. The FT-IR spectra were recorded from KBr pellets in the range of 4000-400 cm⁻¹ on a Bio-Rad FTS-7 spectrometer. Electrospray mass spectrum (ESI-MS) for compound **1** and **2** in *N,N'*-dimethyl sulfoxide (DMSO) solution were obtained on a Thermo LCQ DECA XP apparatus. TG data were obtained on a TG209F3 Tarsus thermogravimetry, with a heating rate of 10 °C min⁻¹ in an N₂ atmosphere. Variable-temperature magnetic susceptibility measurements were obtained to 300 K on poly-crystalline samples using a SQUID magnetometer MPMS XL-7 (Quantum Design) at 0.05 T for **1** and **2**. The magnetization was measured for compounds **1** and **2** at 2 K in the 0-8 T range. The diamagnetic correction for each sample was determined from Pascal's constants.² The effective molar magnetic moments were calculated with the equation $\mu_{\text{eff}} = 2.828(\chi_M T)^{1/2}$.

.

Synthesis of [Dy₁₂(OH)₁₆(phenda)₈(H₂O)₈][Dy(phenda)₂]₂Cl₂·16DMSO·10MeOH·45H₂O (1·16DMSO·10MeOH·45H₂O). Dy(OAC)₃·4H₂O (0.071 g, 0.2 mmol), H₂phendox (0.053 g, 0.2 mmol), H₂phenda (0.014 g, 0.05 mmol) and MeOH/DMSO (12 mL, *V/V* = 5/1) were sealed and heated in a HCl-acidified 23 mL Teflon lined stainless steel autoclave at 120 °C for 6 days. Diamond light yellow crystals of **1**·16DMSO·10MeOH·45H₂O were obtained in a very lower yield. An improved synthetic method for complex **1**·16DMSO·10MeOH·45H₂O was found as followed: Dy(OAC)₃·4H₂O (0.071 g, 0.2 mmol), H₂phenda (0.027 g, 0.1 mmol), two drops dilute HCl and MeOH/DMSO (12 mL, *V/V* = 5/1) were sealed and heated in a 23 mL Teflon lined stainless steel autoclave at 120 °C for 6 days. Diamond light yellow crystals of **1**·16DMSO·10MeOH·45H₂O were obtained (yield: 27 mg, 22.6 % based on Dy). Elemental analysis calcd (Found) for **1**·16DMSO·10MeOH·45H₂O (C₂₁₀H₃₃₀Cl₂Dy₁₄N₂₄O₁₄₃S₁₆): C 30.25 (29.64), H 3.99 (3.90); N 4.03 (4.05)%. IR data (KBr, cm⁻¹): 3396 br, 1616 vs, 1564s, 1463 s, 1429 m, 1396 m, 1363 m, 1305

m, 1269 w, 1175 w, 1018 m, 950w, 877w, 843 m, 743 m, 647 w, 617 w, 591w, 426 w. MS (negative ESI; DMSO) (m/z, %): 696.1(100.0) [Dy(phenda)₂]⁻ ([Figure S1](#)).

Synthesis of [Dy₁₂(OH)₁₆(phenda)₈(H₂O)₈Cl₂](OH)₂·15MeOH·40H₂O (2·15MeOH·40H₂O). Dy(OAC)₃·4H₂O (0.071 g, 0.2 mmol), H₂phendox (0.053 g, 0.2 mmol), H₂phenda (0.014 g, 0.05 mmol), DyCl₃·6H₂O (18 mg, 0.05mmol) and MeOH/DMSO (12 mL, V/V = 5/1) were sealed and heated in a 23 mL Teflon lined stainless steel autoclave at 120 °C for 6 days. Octahedron light yellow crystals of **2·15MeOH·40H₂O** were obtained along with Diamond light yellow crystals of **1** as side-product. An improved synthetic method for complex **2·15MeOH·40H₂O** was found as followed: Dy(OAC)₃·4H₂O (0.071 g, 0.2 mmol), H₂phenda (0.027 g, 0.1 mmol), DyCl₃·6H₂O (18mg, 0.05mmol) and MeOH/DMSO (12 mL, V/V = 5/1) were sealed and heated in a 23 mL Teflon lined stainless steel autoclave at 120 °C for 6 days. Octahedron light yellow crystals of **2·15MeOH·40H₂O** were obtained as single phase (yield 25 mg, 25.8 % based on Dy). Elemental analysis calcd (Found) for **2·15MeOH·40H₂O** (C₁₂₇H₂₂₂Cl₂Dy₁₂N₁₆O₁₁₃): C 26.29 (29.28), H 3.86 (3.84); N 3.86 (3.67)%. IR data (KBr, cm⁻¹): 3313 br, 1617 vs, 1565s, 1466 s, 1430 m, 1397 m, 1311 m, 1182 w, 1019 m, 951w, 878w, 812 m, 765 m, 648 w, 426 w.

X-Ray Crystallography. Suitable single crystals of each complex were carefully selected under polarizing microscope and glued to a thin glass fiber. Diffraction data for compound **1·16DMSO·10MeOH·45H₂O** and **2·15MeOH·40H₂O** were recorded on Rigaku R-AXIS SPIDER Image Plate diffractometer with graphite-monochromated MoK_α radiation ($\lambda = 0.71073 \text{ \AA}$) at 150 (2) K. The structures were solved with direct methods and refined with full-matrix least-squares (SHELX-97). All non-hydrogen atoms were refined anisotropically by least-squares on F^2 using the SHELXTL program.³ Hydrogen atoms on organic ligands were generated by the riding mode.

Because the DMSO molecules are slightly disordered, 37 restraints were used in the refinement of **1**·16DMSO·10MeOH·45H₂O.

For **1**·16DMSO·10MeOH·45H₂O and **2**·15MeOH·40H₂O, the asymmetric unit contains one eighth of Dy₁₂ clusters, one fourth of the uncoordinated chloride and highly disordered lattice aqua molecules. The latter were disordered and could not be modeled properly; thus, program SQUEEZE,⁴ a part of the PLATON package of crystallographic software, was used to calculate the solvent disorder area and remove its contribution to the overall intensity data. A total of 388 parameters for **1** and 225 parameters for **2** were refined in the final least-squares cycle using 1177 reflections for **1** and 1830 reflections for **2** with $I > 2\sigma(I)$ to yield R₁ and wR₂ of 0.0399 and 0.1060 for **1** and R₁ and wR₂ of 0.0337 and 0.0806 for **2**, respectively. Selected bond distances and bond angles are listed in [Tables S1-S2](#).

References:

- 1 C. J. Chandler, L. W. Deady and J. A. Reiss, *J. Heterocycl. Chem.* 1981, **18**, 599.
- 2 F. E. Mabbs and D. J. Machin, *Magnetism and Transition Metal Complexes*, Chapman and Hall, London, 1973.
- 3 *SHELXTL 6.10*, Bruker Analytical Instrumentation, Madison, Wisconsin, USA, 2000.
- 4 P. van der Sluis and A. L. Spek, *Acta Crystallogr., Sect. A: Found. Crystallogr.* 1990, **A46**, 194.

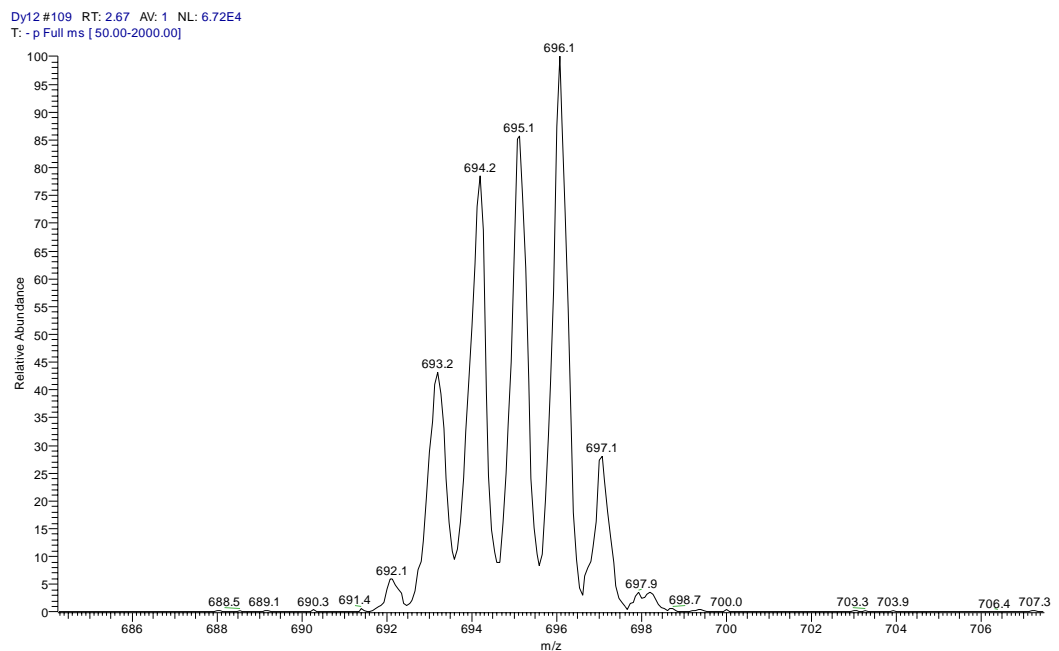


Fig. S1 ESI-MS Spectra for **1**.

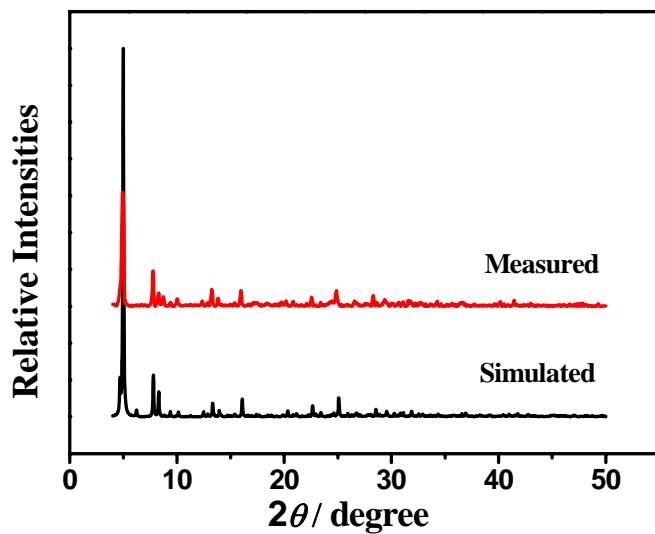


Fig. S2 XRD patterns of **1**

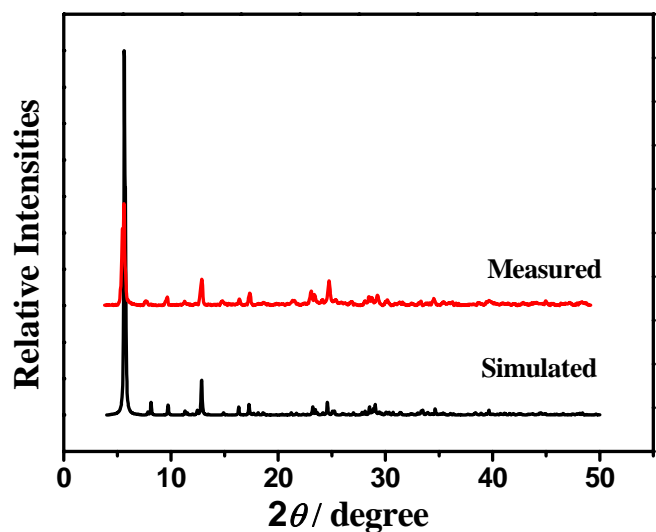


Fig. S3 XRD patterns of **2**

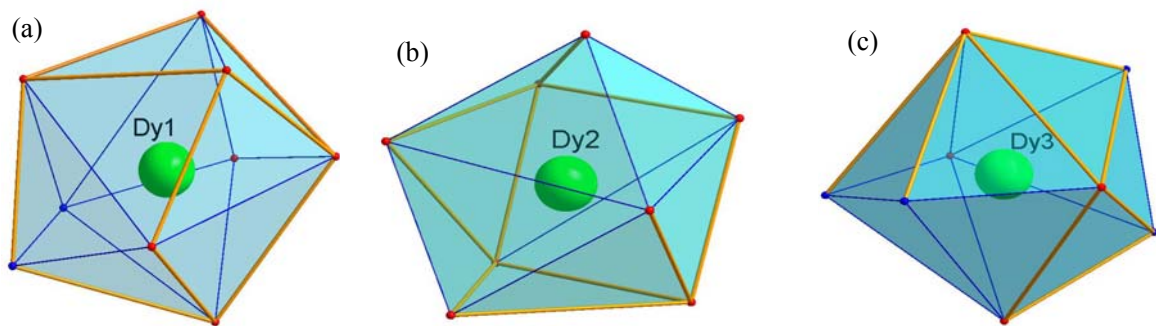


Fig. S4 Coordination polyhedrons of Dy atoms in **1** and **2**.

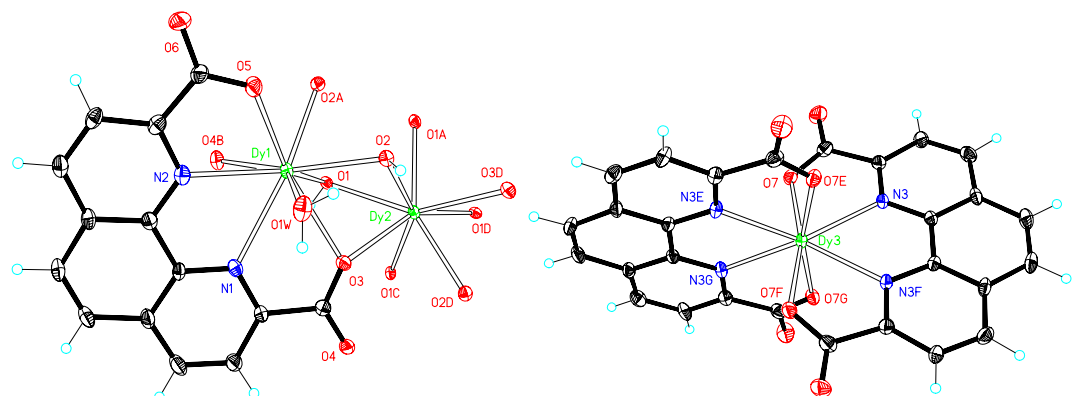


Fig. S5 the coordination environment of the dysprosium atom in **1**.Symmetry codes: a) x,-y+1/2,-z+1/2; b) y,-x+1/2,z; c) -y+1/2,x,z; d)y,x,-z+1/2; e)y-1/2,-x,-z; f) -x-1/2,-y+1/2,z; g) -y,x+1/2,-z; h)-x+1/2,-y+1/2,z.

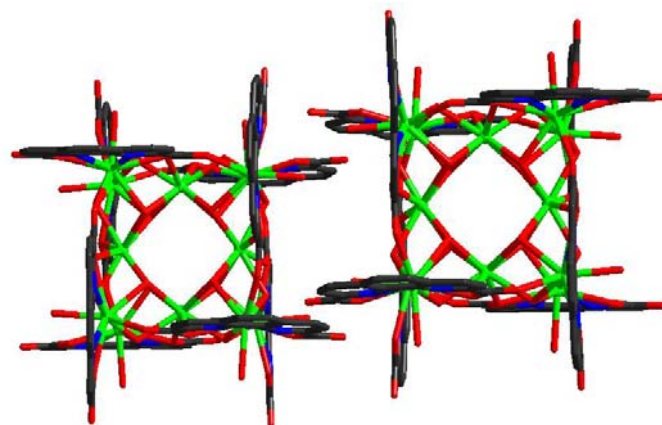


Fig. S6 The off-set $\pi\text{-}\pi$ interaction in the distance of $3.577(8)$ Å between phendox $^{2-}$ groups from the neighboring duodecanuclear units in **1**. The H atoms, chlorides and guest molecules are omitted for clarity.

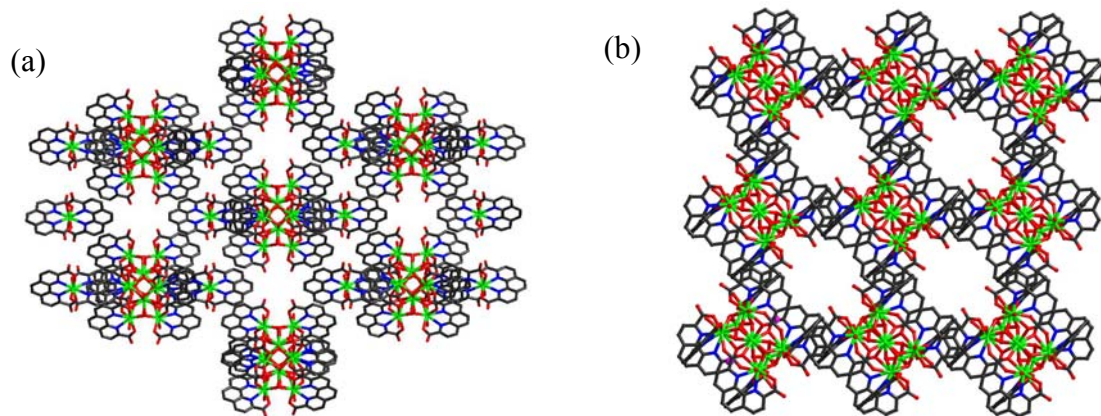
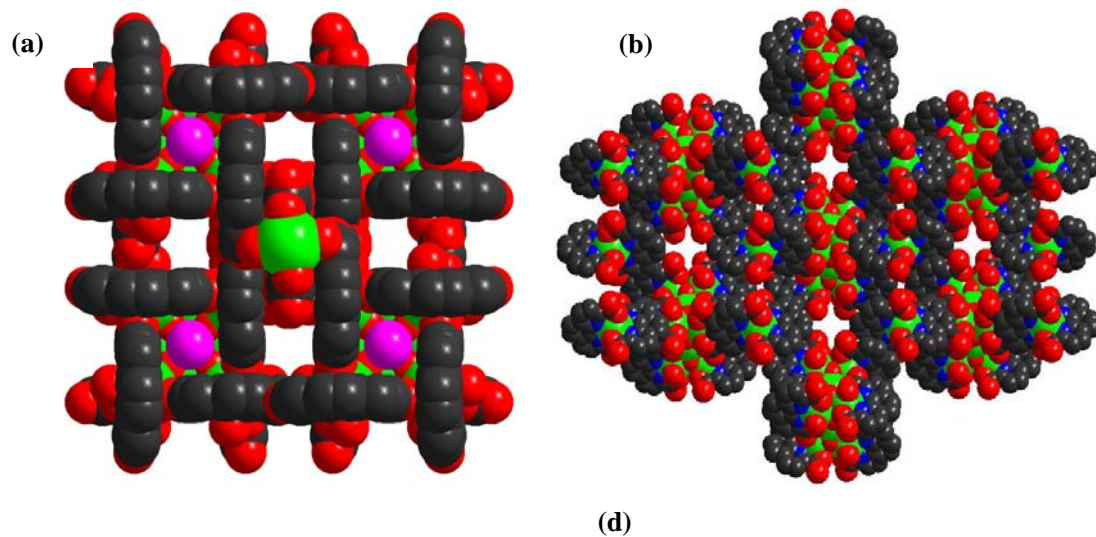


Fig. S7 (a) The supramolecular network of **1** viewed along the *a* or *b*-axis; (b) The supramolecular network of **2** viewed along the *a* or *b*-axis. Green, Dy; red, O; black, C; blue, N; purple, Cl. The H atoms, chlorides and guest molecules are omitted for clarity.



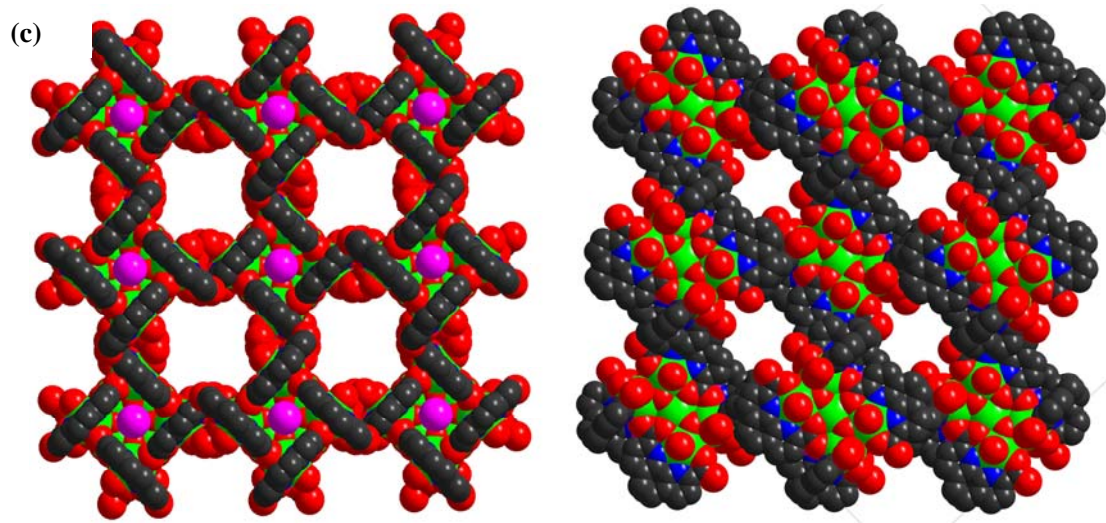


Fig. S8 Space-filling mode of supramolecular network of **1** viewed down from *c* axis (a) and *a* or *b* axis (b). Space-filling mode of supramolecular network of **2** viewed along the *c*-axis (c) and viewed along the *a* or *b* axis (d). The H atoms and guest molecules and in the channels are omitted for clarity. Green, Dy; red, O; black, C; blue, N; purple, Cl.

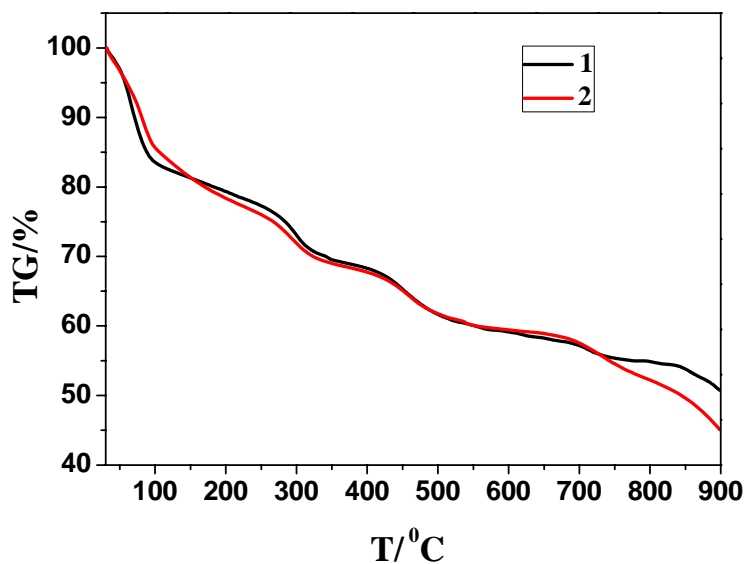


Fig. S9. TG curve of **1-2** under N_2 .

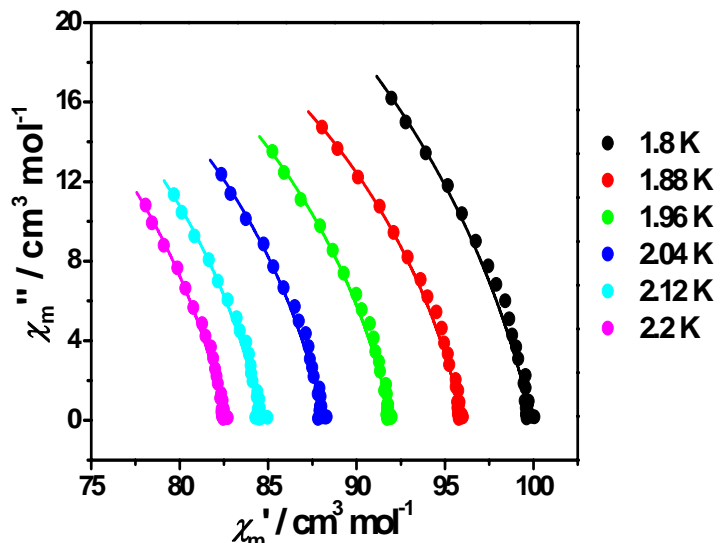


Fig. S10 Cole-Cole plot using the ac susceptibility data for **1**. The solid lines are the best fit obtained with a generalized Debye model (with α always smaller than 0.15).

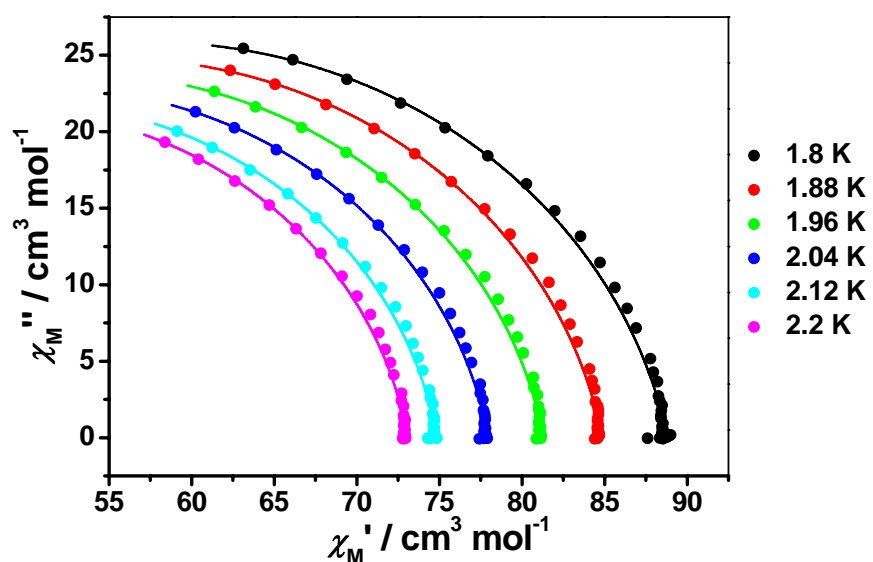


Fig. S11 Cole-Cole plot using the ac susceptibility data for **2**. The solid lines are the best fit obtained with a generalized Debye model (with α always smaller than 0.10).

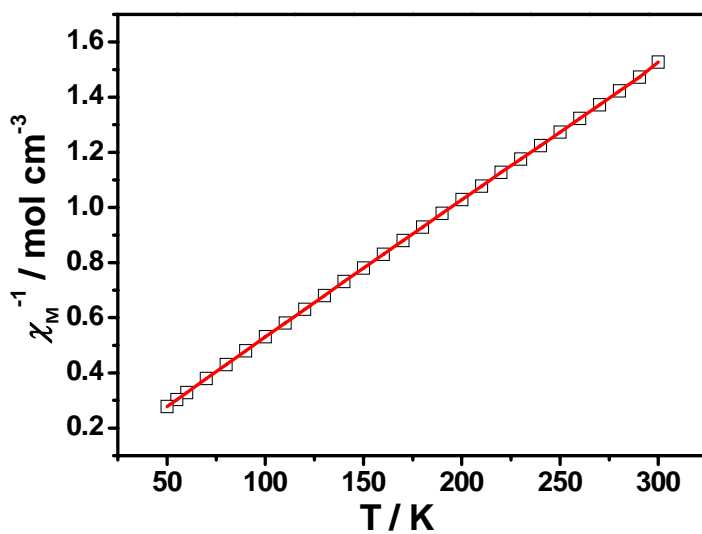


Fig. S12. Plot of Curie-Weiss fitting of χ_M^{-1} versus T curve for **1** at 500 Oe from 50 K to 300 K.

Table S1. Selected bond lengths (\AA) and angles ($^{\circ}$) for **1**.

Dy(1)-O(1W)	2.371(5)	Dy(2)-O(1)	2.382(4)
Dy(1)-O(2)	2.382(4)	Dy(2)-O(1d)	2.382(4)
Dy(1)-O(5)	2.382(5)	Dy(2)-O(3)	2.442(4)
Dy(1)-O(2a)	2.390(4)	Dy(2)-O(3d)	2.442(4)
Dy(1)-O(4b)	2.398(4)	Dy(3)-O(7)	2.335(5)
Dy(1)-O(1)	2.417(4)	Dy(3)-O(7e)	2.335(5)
Dy(1)-N(2)	2.581(5)	Dy(3)-O(7f)	2.335(5)
Dy(1)-O(3)	2.592(4)	Dy(3)-O(7g)	2.335(5)
Dy(1)-N(1)	2.598(5)	Dy(3)-N(3)	2.473(5)
Dy(2)-O(1c)	2.324(4)	Dy(3)-N(3f)	2.473(5)
Dy(2)-O(1a)	2.324(4)	Dy(3)-N(3g)	2.473(5)
Dy(2)-O(2d)	2.346(4)	Dy(3)-N(3e)	2.473(5)
Dy(2)-O(2)	2.346(4)		
O(1W)-Dy(1)-O(2)	76.89(16)	O(1c)-Dy(2)-O(1a)	119.8(2)
O(1W)-Dy(1)-O(5)	79.97(17)	O(1c)-Dy(2)-O(2d)	70.98(15)
O(2)-Dy(1)-O(5)	98.52(15)	O(1a)-Dy(2)-O(2d)	147.01(14)
O(1W)-Dy(1)-O(2a)	127.25(17)	O(1c)-Dy(2)-O(2)	147.01(14)
O(2)-Dy(1)-O(2a)	68.58(18)	O(1a)-Dy(2)-O(2)	70.98(15)
O(5)-Dy(1)-O(2a)	67.64(16)	O(2d)-Dy(2)-O(2)	118.5(2)
O(1W)-Dy(1)-O(4b)	140.46(16)	O(1c)-Dy(2)-O(1)	80.0(2)
O(2)-Dy(1)-O(4b)	142.56(15)	O(1a)-Dy(2)-O(1)	70.19(17)
O(5)-Dy(1)-O(4b)	92.69(16)	O(2d)-Dy(2)-O(1)	141.45(14)
O(2a)-Dy(1)-O(4b)	83.29(15)	O(2)-Dy(2)-O(1)	74.92(14)
O(1W)-Dy(1)-O(1)	136.47(15)	O(1c)-Dy(2)-O(1d)	70.19(17)
O(2)-Dy(1)-O(1)	73.65(14)	O(1a)-Dy(2)-O(1d)	80.0(2)
O(5)-Dy(1)-O(1)	135.33(15)	O(2d)-Dy(2)-O(1d)	74.92(14)
O(2a)-Dy(1)-O(1)	68.69(14)	O(2)-Dy(2)-O(1d)	141.45(14)
O(4b)-Dy(1)-O(1)	73.33(14)	O(1)-Dy(2)-O(1d)	118.6(2)
O(1W)-Dy(1)-N(2)	78.27(16)	O(1c)-Dy(2)-O(3)	81.83(15)
O(2)-Dy(1)-N(2)	151.34(16)	O(1a)-Dy(2)-O(3)	127.38(15)
O(5)-Dy(1)-N(2)	63.04(17)	O(2d)-Dy(2)-O(3)	83.38(14)
O(2a)-Dy(1)-N(2)	117.69(16)	O(2)-Dy(2)-O(3)	68.99(14)
O(4b)-Dy(1)-N(2)	64.08(16)	O(1)-Dy(2)-O(3)	67.50(14)

O(1)-Dy(1)-N(2)	134.99(15)	O(1d)-Dy(2)-O(3)	148.84(14)
O(1W)-Dy(1)-O(3)	74.42(16)	O(1c)-Dy(2)-O(3d)	127.38(15)
O(2)-Dy(1)-O(3)	65.97(14)	O(1a)-Dy(2)-O(3d)	81.83(15)
O(5)-Dy(1)-O(3)	152.41(16)	O(2d)-Dy(2)-O(3d)	68.99(14)
O(2)-Dy(1)-O(3)	121.44(14)	O(2)-Dy(2)-O(3d)	83.38(14)
O(4b)-Dy(1)-O(3)	113.61(15)	O(1)-Dy(2)-O(3d)	148.84(14)
O(1)-Dy(1)-O(3)	64.62(13)	O(1d)-Dy(2)-O(3d)	67.50(14)
N(2)-Dy(1)-O(3)	120.05(16)	O(3)-Dy(2)-O(3d)	124.8(2)
O(1W)-Dy(1)-N(1)	77.60(18)	O(4b)-Dy(1)-N(1)	74.53(16)
O(2)-Dy(1)-N(1)	124.93(16)	O(1)-Dy(1)-N(1)	93.87(15)
O(5)-Dy(1)-N(1)	123.63(17)	N(2)-Dy(1)-N(1)	62.07(18)
O(2b)-Dy(1)-N(1)	155.15(16)	O(3)-Dy(1)-N(1)	60.47(15)
O(7)-Dy(3)-O(7e)	90.89(3)	O(7)-Dy(3)-N(3g)	81.39(17)
O(7)-Dy(3)-O(7f)	165.7(2)	O(7e)-Dy(3)-N(3g)	129.18(17)
O(7e)-Dy(3)-O(7f)	90.89(3)	O(7f)-Dy(3)-N(3g)	86.52(16)
O(7)-Dy(3)-O(7g)	90.89(3)	O(7g)-Dy(3)-N(3g)	65.08(17)
O(7e)-Dy(3)-O(7g)	165.7(2)	N(3)-Dy(3)-N(3g)	135.75(17)
O(7f)-Dy(3)-O(7g)	90.89(3)	N(3f)-Dy(3)-N(3g)	135.75(17)
O(7)-Dy(3)-N(3)	65.08(17)	O(7)-Dy(3)-N(3e)	86.52(16)
O(7e)-Dy(3)-N(3)	81.39(17)	O(7e)-Dy(3)-N(3e)	65.08(17)
O(7f)-Dy(3)-N(3)	129.18(17)	O(7f)-Dy(3)-N(3e)	81.39(17)
O(7g)-Dy(3)-N(3)	86.52(16)	O(7g)-Dy(3)-N(3e)	129.18(17)
O(7)-Dy(3)-N(3f)	129.18(17)	N(3)-Dy(3)-N(3e)	135.75(17)
O(7e)-Dy(3)-N(3f)	86.52(16)	N(3f)-Dy(3)-N(3e)	135.75(17)
O(7f)-Dy(3)-N(3f)	65.08(17)	N(3g)-Dy(3)-N(3e)	64.4(3)
O(7g)-Dy(3)-N(3f)	81.39(17)	N(3)-Dy(3)-N(3f)	64.4(3)

Symmetry codes for **1**: a) x,-y+1/2,-z+1/2, b) y,-x+1/2,z, c) -y+1/2,x,z,d) y,x,-z+1/2, e) y-1/2,-x,-z, f) -x-1/2,-y+1/2,z, g)-y,x+1/2,-z, h) -x+1/2,-y+1/2,z

Table S2. Selected bond lengths (Å) and angles (°) for **2**.

Dy(1)-O(2)	2.369(3)	Dy(2)-O(1a)	2.323(3)
Dy(1)-O(2a)	2.381(3)	Dy(2)-O(1c)	2.323(3)
Dy(1)-O(1W)	2.386(4)	Dy(2)-O(2d)	2.361(3)
Dy(1)-O(5)	2.390(4)	Dy(2)-O(2)	2.361(3)
Dy(1)-O(4b)	2.408(4)	Dy(2)-O(1d)	2.380(3)
Dy(1)-O(1)	2.412(3)	Dy(2)-O(1)	2.380(3)
Dy(1)-N(2)	2.582(4)	Dy(2)-O(3d)	2.435(3)
Dy(1)-O(3)	2.591(3)	Dy(2)-O(3)	2.435(3)
Dy(1)-N(1)	2.602(4)		
O(2)-Dy(1)-O(2a)	68.12(13)	O(1a)-Dy(2)-(1c)	119.97(14)
O(2)-Dy(1)-O(1W)	78.09(11)	O(1a)-Dy(2)-(2d)	147.23(9)
O(2a)-Dy(1)-O(1W)	128.51(12)	O(1c)-Dy(2)-(2d)	70.44(11)
O(2)-Dy(1)-O(5)	97.59(12)	O(1a)-Dy(2)-O(2)	70.44(11)
O(2a)-Dy(1)-O(5)	68.68(12)	O(1c)-Dy(2)-O(2)	147.23(9)
O(1W)-Dy(1)-O(5)	79.06(13)	O(2d)-Dy(2)-O(2)	119.21(16)
O(2)-Dy(1)-O(4b)	142.61(11)	O(1a)-Dy(2)-(1d)	80.65(14)
O(2a)-Dy(1)-O(4b)	84.01(11)	O(1c)-Dy(2)-(1d)	69.71(10)
O(1W)-Dy(1)-O(4b)	139.09(11)	O(2)-Dy(2)-(1d)	74.38(10)
O(5)-Dy(1)-O(4b)	94.67(13)	O(2)-Dy(2)-O(1d)	141.66(9)
O(2)-Dy(1)-O(1)	73.65(10)	O(1a)-Dy(2)-O(1)	69.71(10)
O(2a)-Dy(1)-O(1)	68.62(10)	O(1c)-Dy(2)-O(1)	80.65(14)
O(1W)-Dy(1)-O(1)	136.50(11)	O(2d)-Dy(2)-O(1)	141.66(9)
O(5)-Dy(1)-O(1)	136.53(11)	O(2)-Dy(2)-O(1)	74.38(10)

O(4b)-Dy(1)-O(1)	73.19(10)	O(1d)-Dy(2)-O(1)	118.81(14)
O(2)-Dy(1)-N(2)	150.95(14)	O(1a)-Dy(2)-(3d)	82.00(10)
O(2a)-Dy(1)-N(2)	117.50(13)	O(1c)-Dy(2)-(3d)	127.06(11)
O(1W)-Dy(1)-N(2)	77.36(13)	O(2d)-Dy(2)-(3d)	69.11(10)
O(5)-Dy(1)-N(2)	62.59(14)	O(2)-Dy(2)-O(3d)	83.55(11)
O(4b)-Dy(1)-N(2)	64.30(13)	O(1d)-Dy(2)-(3d)	67.59(10)
O(1)-Dy(1)-N(2)	135.40(13)	O(1)-Dy(2)-O(3d)	148.53(10)
O(2)-Dy(1)-O(3)	66.36(10)	O(1a)-Dy(2)-O(3)	127.06(11)
O(2a)-Dy(1)-O(3)	121.37(10)	O(1c)-Dy(2)-O(3)	82.00(10)
O(1W)-Dy(1)-O(3)	74.02(12)	O(2)-Dy(2)-O(3)	83.55(11)
O(5)-Dy(1)-O(3)	150.89(12)	O(2)-Dy(2)-O(3)	69.11(10)
O(4b)-Dy(1)-O(3)	112.91(12)	O(1d)-Dy(2)-O(3)	148.53(10)
O(1)-Dy(1)-O(3)	64.63(9)	O(1)-Dy(2)-O(3)	67.59(10)
N(2)-Dy(1)-O(3)	120.38(13)	O(3d)-Dy(2)-O(3)	124.79(16)
O(2)-Dy(1)-N(1)	125.69(13)	O(4b)-Dy(1)-N(1)	73.46(13)
O(2a)-Dy(1)-N(1)	154.93(13)	O(1)-Dy(1)-N(1)	93.91(12)
O(1W)-Dy(1)-N(1)	76.55(13)	N(2)-Dy(1)-N(1)	62.25(15)
O(5)-Dy(1)-N(1)	123.09(13)	O(3)-Dy(1)-N(1)	60.78(12)

Symmetry codes for **2**: a)y,x,-z+3/2; b) y,-x+1/2,z; c) -y+1/2,x,z ; d) -x+1/2,y,-z+3/2